Development of Dynamic Discharge Arc Driver with Computer-Aided Circuit Simulation

Robert E. Dannenberg*
NASA Ames Research Center, Moffett Field, Calif.
and
Petar I. Slapnicar †
University of Split, Split, Yugoslavia

Higher shock speed performance of an arc-driven shock tube has been obtained with the use of a dynamic discharge arc driver (DDAD). In DDAD operation, the driver gas mass is fed continuously into the arc chamber during the discharge. DDAD operation is shown to increase the power to the arc chamber by raising the arc resistance throughout the entire discharge period. The time-varying arc resistance is calculated by a computer program (SPARK) designed to model the electrical discharge performance of the energy storage and driver system. Effects of various design and operating parameters of the arc driver on the overall facility performance are analyzed with the aid of the SPARK program. The DDAD operation uses hydrogen as the driver gas to generate in air shock Mach numbers in excess of 60. Shock speeds of 42 km/sec were obtained in H_2/He mixtures.

Introduction

ELECTRICALLY heated, arc-driven shock tubes have played a major part in the development of entry technology. Through development, particularly of conical-shaped arc chambers, the arc driver has reached a high level of performance in its capability for generating strong shock waves.[1,2] However, the most severe velocity simulation requirements for a hypersonic vehicle traversing a cloud of water droplets in the Earth's atmosphere or for a Jupiter entry were beyond the capabilities of conventional driver performance. Attempts to increase the maximum attainable shock speed by further raising the power level in the arc chamber generally have been unsuccessful. At the higher levels of operation, i.e., with the arc energy approaching several hundred kilojoules, the shock velocity no longer improved significantly as bank energy increased. In fact, measurements indicated that the shock speed actually decreased.

To understand and predict the loss mechanisms causing the difficulties just noted requires knowledge of the transient behavior of the power dissipation in the various components comprising the driver electrical system. Attempts to analyze the behavior of the circuit elements by simple fixed resistance inductance capacitance (RLC) components were found to be unacceptably inadequate.

A computer program (designated SPARK) using nonlinear RLC circuit analysis was developed to model the transient electrical discharge performance of the Ames 1-MJ energy storage and arc driver facility. The instantaneous voltage drops and energy absorption characteristics of the circuit components are computed utilizing the time history of the circuit current as input data. The program provides a significant new ability to determine the arc resistance as a function of time during the discharge period. Furthermore, the program is valuable in relating the actual energy discharged within the arc chamber to shock speed measurements.

Additionally, the SPARK program enables new analysis of previously recorded electrical discharge data. A number of experimental circuit current records for different arc chamber arrangements were reprocessed and analyzed by the use of the program. These results, together with their shock speed data, indicated that achievement of the best possible energy transfer to the arc chamber and the highest shock-tube performance depended on 1) an adequate mass flow rate of driver gas, and 2) maximization of arc resistance.

External injection of driver gas into the arc chamber during the period of the arc is one method of achieving both a higher electrical resistance and an increased mass flow time. With only minor modifications to existing facility equipment, a conical arc driver was adapted to incorporate a rapid gas injection system. This modified driver, designated a dynamic discharge arc driver (DDAD), uses continual mass injection of driver gas during the discharge to maintain a higher chamber pressure during the period of the arc. Also, the gas injection system is arranged to initiate the discharge of the capacitor bank. Test results are presented for DDAD operation in air at high shock Mach numbers from 1 to 380 Torr and in a 0.95 H_2-0.05 He mixture at 1 Torr. It was found that the use of mass addition increased the shock tube performance, allowing higher pressure and velocity limits. The numerical model is discussed briefly; the calculations performed are described; and the agreement between experimental data and SPARK calculations is shown.

Computer Program for Transient Discharge

The SPARK program was developed to model the electrical network of a complete electrically heated driver and energy storage system for hypervelocity or planetary entry types of shock tubes. The components or elements of the energy storage system generally consist of a capacitor bank coordinated with coaxial cabling to a collector assembly at the driver. The bank may be fused or not. Network equations were written based on Kirchhoff's Current Law for each of the elements in the circuit (i.e., nodal analysis). The solution of the integral differential circuit equations used implicit numerical integration techniques developed for computer-aided circuit analysis.[3] For convenient data analysis, SPARK was programmed for two stages of computations. The first calculates voltages, power and energies absorbed by elements in the circuit in response to a specified current wave form. The second calculates arc resistance. The program was written in FORTRAN IV language for a Digital Equipment Corporation PDP-8/e computer.

Presented as Paper 75-176 at the AIAA 13th Aerospace Sciences Meeting, Pasadena Calif., Jan. 20-22, 1975; received Sept. 25, 1975; revision received Feb. 17, 1976.

Index categories: Computer Technology and Computer Simulation Techniques; Shock Waves and Detonations; Research Facilities and Instrumentation.

*Research Scientist, Associate Fellow AIAA.

†Associate Professor, Electrical Engineering; also Fulbright Scholar, Stanford University, August 73-74.

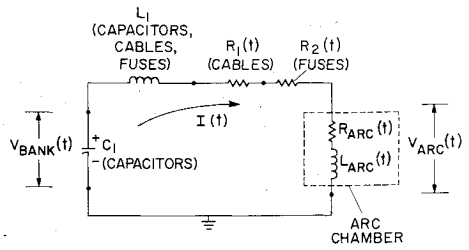

Fig. 1 Equivalent electric circuit with arc model.

The energy storage, cabling, and driver systems represent a series electrical circuit of capacitance *C1*, resistance of cables *R1*, resistance of fuses *R2*, and inductance *L1* (capacitor bank, fuses, and cables), and the unknown arc impedance. Both *R1* and *R2* increase with time due to ohmic heating of the conductors. The program calculates the increase in these resistances with current flow, as well as the temperature rise in the conductors. Modeling the system to an equivalent circuit network is straightforward, as indicated in Fig. 1.

A convenient feature of the SPARK program is that the first stage calculations are made independent of any knowledge of the inductance and resistance within the arc chamber. The voltage drop across the arc chamber, V_{arc}, is calculated from the bank potential less the sum of the potential differences across each of the know circuit elements as expressed by

$$V_{arc}(t) = V_{bank}(0) - \left[\frac{1}{C1}\int_0^t I(t)\,dt + V_{L1}(t) + V_{R1}(t) + V_{R2}(t)\right] \quad (1)$$

Similarly, the arc energy, as a function of time, is computed from the difference between the bank energy and the energies absorbed in known elements. Other program outputs, tabulated or plotted, include the energies absorbed in the cabling and fuses; the temperature rise and resistance increase in the cables and fuses; the rate of change of circuit current with time, dI/dt; and values of the arc inductance for times at the zero current crossings for use in the second stage of the program. An equilvalent arc resistance R^*_{arc}, also is calculated based on the total energy discharged in the arc chamber. It is a well-known fact that , in the circuit shown in Fig. 1, each resistive circuit element will absorb a portion of the preset stored bank energy, the amount being directly proportional to the value of the individual resistance. For the present purpose,

$$R^*_{arc} = [R1+R2]\left[\frac{E_{arc}}{E_{preset}-E_{arc}}\right] = E_{arc}\Big/\int_0^\infty I^2(t)\,dt \quad (2)$$

where R^*_{arc} is computed using the latter expression of Eq. (2). This resistance is a useful diagnostic tool for evaluating changes in the arc properties and for comparison of electrical performance with shock speed measurements.

In the second stage of the program, the arc resistance is calculated for the arc modeled by circuit elements consisting of a series connection of a time-varying inductance and resistance (Fig. 1). For this circuit arrangement, the voltage drop across the arc chamber is given by the relationship

$$V_{arc} = R_{arc}(t)I(t) + (d/dt)\,[L_{arc}(t)I(t)] \quad (3)$$

Values of V_{arc}, I, and dI/dt were derived in first-stage calculations. The arc resistance $R_{arc}(t)$ is computed from Eq. (3) predicated on the values of arc inductance as derived from the recorded shape of the particular current time record. At the initiation of the arc current rise, $t(0)$, and at subsequent times (with an oscillatory discharge) as the current value passes through zero, the value of L_{arc} is determined from

$$V_{bank} = (L1+L_{arc})\,(dI/dt) \quad (4)$$

Selecting a curve encompassing the values of arc inductance derived from Eq. (4) establishes $L_{arc}(t)$. After the determination of L_{arc} values, they are entered, and the program completes the computations of the arc resistance.

The SPARK program requires, as input data, the values of the known electrical circuit elements, the mass of the copper cabling and fuses, the preset voltage of the capacitor bank, and the circuit current (arc discharge record). The current record must be obtained by experiment. Its shape, determined by the time-varying circuit parameters, provides the basis for information of the arc inductance. The circuit current also is affected by the geometry of the driver, as well as the preset conditions within the arc chamber (type of gas, pressure, trigger wire, etc.). The $I(t)$ record is converted from its original analog format to a digital form using second-order polynomial interpolation.

Application of Program Calculations

At the Ames Research Center, the 20/40-kV energy storage system used to power the arc-heated shock-tube drivers is a capacitor bank capable of storing 1 MJ when charged to its rated voltage. By switching the bus bars on the bank, the capacitor groups can be connected either in a series-parallel 0- to 40-kV mode (1320 μF), or in a parallel 0- to 20-kV mode (5280 μF). Description of the capacitor bank, cabling, and fuses is given in Ref. 4. An example of the SPARK program results is shown in Fig. 2 for the Ames energy storage system and a conical driver similar to that described in Ref. 2. The capacitor bank was in the 20-kV mode. The element values for the known components in the circuit were $C1=5280$ μF, $L1=0.238\mu$H, $R1=2.32$ mΩ, and $R2=0.083$ mΩ. The initial load pressure in the arc chamber was 2 atm hydrogen. With this driver, the trigger wire was pulled toward the charged electrode until the wire exploded to strike the arc.

Figure 2a shows the record of the circuit current for a discharge with a preset voltage of 15.5 kV. The energy stored in the capacitor bank was 634 kJ. The current curve is reproduced starting at the beginning of the discharge. The dwell period[5] following the explosion of the trigger wire prior to the arc discharge is not graphed, as it is not pertinent to this discussion. The decay in the bank voltage during the discharge period is indicated in Fig. 2b. Voltage measurements at the bank agreed with the calculated values. For clarity, experimental points were shown only at 25-μsec intervals.

Prior to the arc discharge, the voltage of the charged electrode in the arc chamber equals that of the preset bank voltage. At the instant of discharge, the combined circuit impedance, fixed plus unknown arc components, acts to reduce the arc voltage abruptly, as shown in Fig. 2b. The voltage of the electrode in the arc chamber dropped instantly to 8.8 kV, in constrast to the bank value of 15.5 kV. Measurements from a probe positioned at the driver elelctrode agreed with the SPARK calculations both in the initial change and the subsequent voltage decay. The maximum arc voltage is important in several respects. It shows that the applied voltage gradient (volts per centimeter) along the chamber was below the value determined on the basis of the preset conditions. Also, it is indicative of the fact that a sizable portion of the bank energy was dissipated elsewhere in the circuit. Calculations indicated that only 456 kJ, or about 72% of the bank energy, were transferred to the arc chamber. The resistance of the coaxial cabling accounted for the main reduction in the energy available for the arc. Fuse losses were small, less than 7 kJ. The calculated rise in temperature of the fuse wires was 48.3°K, with a change in fuse wire resistance from 0.083 to 0.101 mΩ. The corresponding temperature increase in the coaxial cabling was 10.1°K. The calculated increase in cable resistance was about 0.01 mΩ.

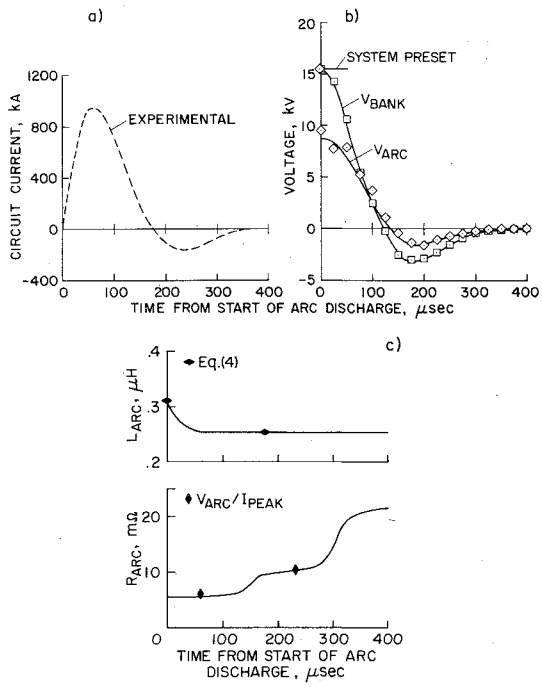

Fig. 2 a) Current and b) voltage characteristics of a 15.5-kV hydrogen discharge in a conical arc driver; c) arc impedance characteristics derived from the computer program. Solid lines represent program calculations. Experimental result: —, □ V_{bank}, ◇ V_{arc}.

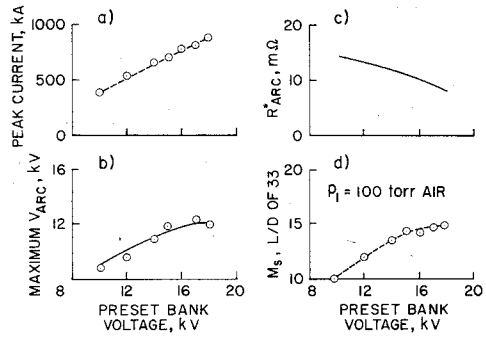

Fig. 3 Variation of performance characteristics with preset bank voltage for conical driver with pull-type trigger wire. Solid lines represent program calculations. Dashed symbols represent experimental results.

As noted earlier, values of arc inductance were calculated at times in the discharge period when the current is zero. These values are indicated in Fig. 2c, together with the selected timewise inductance distribution. As shown here, the arc inductance started typically at a few tenths of a microhenry and decayed to a lower value during the early stage of the discharge. The reduction of inductance with time is consistent with the physical interpretation that the arc diameter is small at arc initiation and increases with the current flow until it fills the chamber.[6] The corresponding calculations for the arc resistance are shown in the lower part of the figure. During the initial current rise, the resistance is low and relatively constant. As the current peaks and decreases, the resistance tends to rise. Following a zero crossing, the arc restrikes, the current again becomes relatively high, and the resistance tends to remain constant. As the current extinguishes, the resistance again increases. The resistance values uniquely determined by V_{arc}/I_{peak} at the maximum positive and negative peak currents are denoted by solid symbols. The equivalent arc resistance R^*_{arc} was 6.2 mΩ. Note that its value lies between those for the maximum positive and negative peak currents. The test was made with 10 Torr of dry air in the driven tube. The measured shock Mach number was 19 at a station 5 m (16.4 ft) downstream of the diaphragm in the 10.16-cm (4-in.)-diam. driven tube.

The discussion so far has demonstrated the capabilities of SPARK computations to determine the properties of a triggered arc discharge as an electrical circuit element. Consideration now will be given to the application of computations that help to explain several areas of driver performance not quantitatively accounted for previously.

For a given facility, the effectiveness of introducing the electrical energy into the driver gas is basically a function of the inital gas load pressure in the arc chamber and the applied voltage. The program results have shown that the external energy losses can be reduced by increasing the load pressure in the chamber. For example, in connection with the data of Fig. 2, an increase in the chamber pressure from 2 to 8.84 atm resulted in a change in the ratio of the arc chamber energy to bank energy from approximately 0.72 to 0.85. The measured circuit current decreased. Calculations confirmed by measurement indicated that the maximum arc voltage was increased from approximately ½ to ¾ that of the preset bank voltage. Shock velocities were higher. With 10 Torr of air in the driven tube, the measured shock Mach number increased from 19 to 24 at the same test station. The equivalent arc resistance also increased, as indicated by a change in R^*_{arc} to 12.9 from 6.2 mΩ. Accurate assessment of the gas temperatures and pressures is difficult because of the complexity of the processes involved in the arc heating. It would appear that higher driver load pressures act to reduce the specific energy (kilojoules per gram) of the gas, a condition considered advantageous for reducing losses due to gas radiation cooling.[5,7]

The increase in shock speed with higher chamber energy is understandable. However, the magnitude of the current peak in Fig. 2a was decreased from 961 to 689 kA because of the increase in load pressure. Previously it has been assumed that a decrease in peak current necessarily would cause a decrease in gas temperature and, hence, a decrease in shock speed, which would be in contradiction to the preceding results. Such an assumption is therefore invalid.

One of the major deficiencies observed in contemporary arc-driven facilities has been a marked reduction in the rate of increase in the shock-tube performance with increased bank voltage. Changing the preset bank voltage is the simplest and most commonly used procedure for varying the energy input into the arc chamber. Effects of raising the preset bank voltage are shown in Fig. 3. The chamber load pressure for the tests was 8.84 atm hydrogen. Increasing the bank voltage increased the circuit current by near straight-line increase in the peak current, as noted in Fig. 3a. The maximum arc voltages, however, tended to level off at the higher preset voltages, as shown in Fig. 3b by both calculations and the experimentally determined values. The calculated arc resistance decreased (Fig. 3c). As the effective arc resistance decreased with respect to the fixed-resistance components, the driver efficienty decreased. The end result of increasing the preset bank voltage in terms of facility performance was, therefore, a reduction of the generated shock speed from the near-linear increase in velocity characteristics noted at lower bank potentials (Fig. 3d).

Data previously reported[5] for arc drivers with cylindrically shaped arc chambers, together with current records available from other facilities, were reprocessed by the SPARK program. These results indicated that longer arcs, ¾ to 3 m in length, had higher resistances than observed for conical chambers. Marked dependence of the arc resistance on the arc length was noted, especially for similar chamber environment (gas, pressure). Increases in arc resistance, as a result of trigger wire geometry,[8] also were noted. The triggered arc behaved as an electrical conductor whose resistance increased almost directly with its length. A value of R^*_{arc} of 0.4 mΩ/cm of arc length (hydrogen driver gas) can be used in circuit calculations for estimating purposes. With the longer driver

chambers, the arc voltages and energies approached those of the capacitor bank, as would be expected. However, the energy densities (joules per cubic centimeter) were less in the larger volume chambers, which generally accounts for the slower shock speeds found with the cylindrical chambers as compared to the shorter conical chambers.

The examination of the long- and the short-arc data in comparison to their measured shock velocities for related test arrangements or conditions indicated that an increase in the arc energy generally showed a perceptable degree of improvement in the shock velocity. All of the results indicate that, in order to obtain the highest possible shock speed, the arc resistance must be maximized. In addition, the mass of gas within the arc chamber must be sufficient to develop the pressure (density) behind the generated shock wave for an adequate test time.

Operational Characteristics of DDAD

The dynamic discharge arc driver (DDAD) utilizes mass addition of the driver gas to improve driver performance by increasing the resistance of the arc and rate of mass flow from the chamber. In DDAD operation, the arc chamber is not filled with gas until the capacitor bank is charged to its preset voltage. When the bank reaches the preset voltage, the rapid gas loading system is activated, controlling the following sequence: filling the arc chamber, bursting the diaphragm, and exploding the trigger wire that initiates the arc discharge. As the gas heats and expands, the density within the chamber tends to decrease. The continual mass addition not only acts to offset the decrease, but also serves to increase the arc resistance because of its cooling effect. Thus, the added gas acts as a thermal-controlling variable resistor. This added resistance provides for circuit damping without significantly affecting the initial rate of rise of the current. Furthermore, the electrical energy is discharged into a moving gas, a condition considered to be more efficient in producing strong shock waves than heating gas at rest.[9,10]

The chamber of the conical arc driver modified for DDAD operation consists of the hollow frustum of a Teflon cone, 17.3 cm long, with base diameters of 2.6 and 10.17 cm, with a 3.2-cm straight-sided section capped by a 1.4-mm-thick Mylar diaphragm. The DDAD is shown in Fig. 4. A new port for the gas-injection system (12.7 mm diam) is located in the straight-sided section. Various components for the storage and control of the gas to be injected into the arc chamber were added to the gas supply sytem leading to the new port. These include a system value, a small-volume high-pressure tank, a remote-controlled valve, a flexible pressure line, and a burst disk assembly. The latter is located as close to the arc chamber as the flange structure permits. The arrangement of the various components is indicated in Fig. 5. The volume of the storage system (system valve to burst disk) is about five times that of the arc chamber. The storage system is pressurized in the following sequence. The gas pressure in the line from the disk to the remote-controlled valve is loaded to 85% of the rated pressure of the burst disk. This valve then is closed, and the pressure in the tank section is loaded to 70 atm hydrogen. The system valve is closed, and the gas injection system is ready for operation.

The DDAD is compact and easily disassembled for cleaning and replacement of the trigger conductor and diaphragm; turnaround time per run is about 3 hr. The driver is fastened to the driven-tube section by means of a rapid-action three-point pneumatic/hydraulic clamping assembly. This assembly (not shown) also serves as the ground return path for the electrical circuit. The coaxial cables from the capacitor bank tie into the current collector assembly as previously described.[4] The high-voltage assembly is insulated with Lexan insulating elements and is brought into the arc chamber through a quarter-turn stainless-steel breech plug. To prevent electrical arcing to the metal walls during the discharge phase, the chamber section is fabricated from a dielectric material. The electrode and trigger wire assembly is checked for electrical isolation with a high-voltage tester to 10 kV over that required for the particular run. This check verifies that the diaphragm provides the necessary standoff protection to prevent premature breakdown, and thus minimizes the change of an arc occurring before the proper preset voltage is attained. After the high-voltage test has been made, a copper bus plate is installed to connect the electrode assembly to the inner collector assembly.

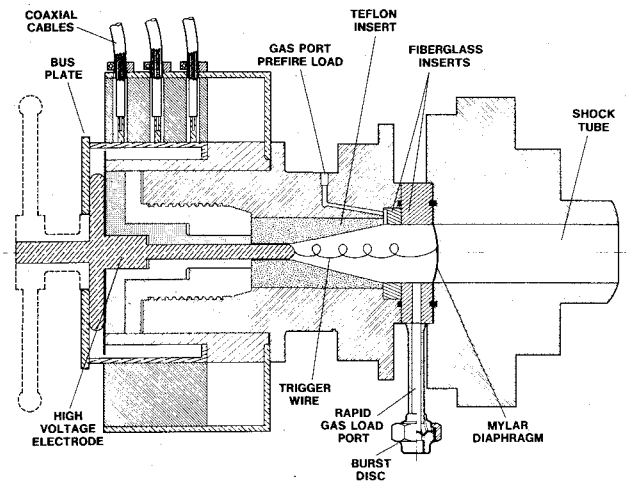

Fig. 4 Assembly of DDAD with 10.16-cm-diam shock tube.

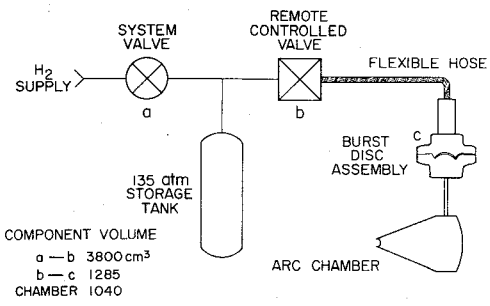

Fig. 5 Arragement of rapid gas load system for DDAD operation.

The arc is initiated within the insulated chamber by means of a fine trigger wire. On installation, one end is fastened to the high-voltage electrode. The wire is coiled loosely along the chamber. Its other end is positioned and attached at the center of the Mylar diaphragm. The run cycle is begun by purging and filling the arc chamber with 2-3 atm of hydrogen through the "prefire" port indicated in Fig. 4. The capacitor bank and trigger wire are charged to the preset voltage. In a programmed sequence, the remote-controlled valve in the gas storage system is opened. The higher-pressure gas stored in the tank section increases the gas pressure in the section of the line behind the disk. The disk permits the gas pressure to build to its rupture valve, at which time it bursts. Abruptly, hydrogen enters the arc chamber, raising the pressure and bursting the Mylar diaphragm. The disintegration of the diaphragm induces voltage breakdown between the charged trigger wire and ground; the wire explodes and initiates the arc discharge. Gas continues to enter the arc chamber at nearly constant pressure from the supply system for several milliseconds.

Experimental Results

With the energy storage system in the 20-kV mode, tests were conducted with the DDAD driver combined with a 10.16-cm-diam driven tube. The initial pressure P_1 was varied from 1 to 380 Torr of dry air. The preset voltage of the bank was varied from about 8 to 14 kV, and a 0.25-mm stainless-steel trigger wire was used in arc initiation. The disk in the injection system was rated to burst at 40 ± 2 atm. The arrival of

the incident shock wave at several stations along the driven tube was determined by means of photomultipliers[11] and wall-mounted twin-electrode ionization probes.[12] The electronic circuitry of both detection systems has been improved for operation at higher shock speeds where precursor ionization is a prominent characteristic of the test gas. A preset threshold-biasing arrangement provides a trigger pulse when the output signal from either type of detector is greater than that of the precursor level. In most cases, only one run was needed to adjust the instrument properly for a particular set of operating conditions. The mass flow rate into the arc chamber would be derived best from the ratio of the injection supply to the chamber pressures. At present, these pressures are difficult to determine under discharge conditions because of the complexity of the arc environment. Undoubtedly, the pressure rise of the arc-heated gas reaches and probably exceeds that of the injection supply during a portion of the discharge period. Of course, no gas would be added during this time. In fact the line is backfilled momentarily. Furthermore, the initial shock-tube loading pressure also plays a part in the pressures developed by the driver. Based on the preceding considerations (and bench test measurements), the mass of gas injected from the start of the pressurizing phase before the diaphragm breaks to the end of the discharge period was calculated to be from nearly double (for P_1 of 380 Torr) to five times (for P_1 of 1 Torr) that used formerly with the arc initiated by means of the pull-wire trigger technique. Although the gas addition was small, it was sufficient to affect the arc characteristics and improve the shock speed. Measurement showed that the maximum arc voltage was increased from about 0.8 (pull-wire operation) to 0.9 that of the preset value. SPARK program calculations indicated that the arc energy and equivalent resistance increased by several percent.

Figure 6 shows the shock-driving capability obtained from preliminary DDAD operation using hydrogen as the driver gas and air as the driven gas. The shaded area in the figure indicates the range previously achieved with the cylindrical, metal diaphragm drivers[13] and conical drivers using pull-wire operation.[14] Performance of the former was limited by excessive heating in the chamber before the diaphragm opened whereas the latter was restricted by the allowable voltage overshoot of the capacitors. The demonstrated increase in the incident shock Mach number represents a practical enhancement of facility performance.

DDAD operation to date has been achieved using about half of the available bank energy storage. The shock-driving ability eventually should be limited by practical electrical considerations or the structural limitation of the shock tube (400 atm). It does not appear that we are close to such limits.

Test times in air were measured from collimated photomultiplier records and by image converter photographs, as described in Ref. 2. Results showed that the test time increased slightly with driven-tube pressure. Test times of 4–5 μsec were observed at a shock Mach number of 61 (P_1 of 1 Torr) and about 20 μsec at a Mach number of 15 (P_1 of 380 Torr).

The attained level of performance with DDAD operation is compared with mission requirements in Fig. 7. Two particular missions are indicated in the figure. One is concerned with the problem of hypersonic vehicles exposed to an atmospheric water-vapor enviroment. Studies of the interaction of shock waves with water droplets or ice crystals for shock velocities of 3 to 7 km/sec into 100 to 300 Torr of air are of interest. As seen from the figure, such conditions are achieved by the DDAD-driven shock tube. Another research area of interest requiring a high-performance arc driver is that for outer planetary atmosphere entry. For Jupiter entry, the most severe, the driven gas is a predominantly hydrogen mixture requiring shock velocities of 40 to 50 km/sec into about 1 Torr of the test gas. The chamber pressure requirements are considerably lower for the lighter test gas,[15] as indicated in

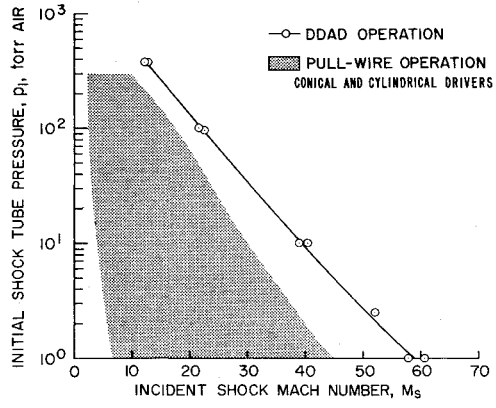

Fig. 6 Performance capability of the Ames DDAD shock tube.

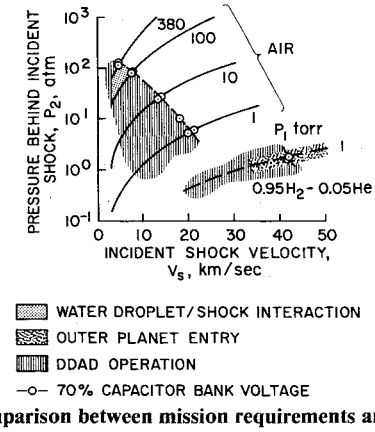

Fig. 7 Comparison between mission requirements and attained level of performance.

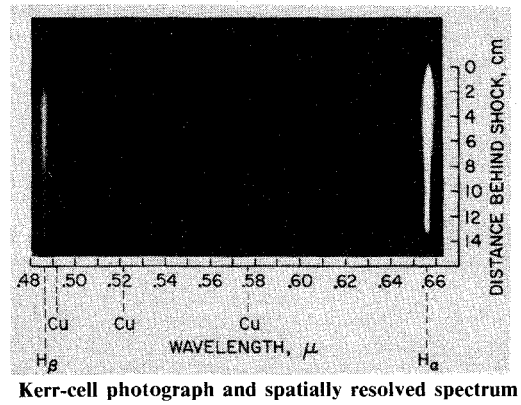

Fig. 8 Kerr-cell photograph and spatially resolved spectrum of the shock-tube flow, shock velocity of 38 km/sec.

Fig. 7. Shock velocity up to 42 km/sec have been produced into the H_2/He mixture.

Narrow passband radiometers[11] and a Kerr-cell shuttered f/1.5 stigmatic spectrograph[16] were used to determine the duration and purity of the H_2/He test gas. These instruments had been used previously with explosively driven shock tubes.[17] Measurement of the test periods were made by David M. Cooper of the Ames Research Center. A typical photograph of the spatially resolved spectrum of the emission behind the shock wave is shown in Fig. 8. The prominent features to be observed in the spectrum are the H_α and H_β lines at 6563 and 4861 Å, respectively. These lines reveal a rapid increase in intensity to a constant level followed by region of decreased intensity. Approximately 7¼ cm behind the shock wave, the radiation intensity decreases, signaling the arrival of the interface between the test and driver gases. At the same spatial location, the first sign of an impurity line, CuI, can be detected. The usable test time was evaluated as 1.9 μsec. The corresponding radiometer measurement for test

time was 2.2 μsec. As expected, the test times increased as shock speed decreased. For a shock velocity of 30.4 km/sec, the test times were 2.7 μsec (spectrograph) and 3.0 μsec (radiometer).

Concluding Remarks

Experimental results of the dynamic discharge arc driver demonstrate that the DDAD concept using mass addition to the driver gas offers a significant improvement in the generation of strong shock waves when compared to conventional arc drivers. The highest rate for external mass injection without adverse effects has not been established yet. DDAD operation produces strong shock waves with sufficient test times for studies of hydrometeor/shock interaction phenomena in air, as well as the simulation of probe entry into atmospheres of the outer planets.

The SPARK computer program, which led to the development of the DDAD, was particularly useful in determining the voltage and energy dissipation in the various components of the electrical system. Heretofore, the literature indicated that the preset bank voltage and its stored energy were the cirteria used in evaluating arc chamber performance in comparison with shock speed. SPARK calculations of new experimental data, as well as the reprocessing of older work, show that the differences between bank and arc values are of utmost significance, particularly for systems with short conical or cylindrical chambers, or for systems with long lengths of cabling between the capacitor bank and the arc driver. As a result, arc energy date should be evaluated carefully before their use.

References

[1]Menard, W. A., "A Higher Performance Electric-Arc Driven Shock Tube," *AIAA Journal*, Vol. 9, Oct. 1971, pp. 2096–2098.

[2]Dannenberg, R. E., "A Conical Arc Driver for High Energy Test Facilites," *AIAA Journal*, Vol. 10. Dec. 1972, pp. 1692–1694.

[3]McCalla, W. J. and Pederson, D. O., "Elements of Computer-Aided Circuit Analysis," *IEEE Transactions on Circuit Theory*, Vol. CT-18, Jan. 1971,. pp. 14-26.

[4]Dannenberg, R. E., and Silva, R. S., "Exploding Wire Initiation and Electrical Operation of 40-kV System for Arc-Heated Drivers up to 10 Feet Long," NASA TN D-5126, April 1969.

[5]Dannenberg, R. E. and Silva, R. S., "Arc Driver Operation for Either Efficient Energy Transfer or High-Current Generation," *AIAA Journal*, Vol. 10, Dec. 1972, pp. 1563–1564; NASA TM X-62,162, 1972.

[6]Livingston, F. R., and Menard, W. A., "Toward Understanding the Conical Arc-Chamber Driver," *Recent Developments in Shock Tube Research, Proceedings of the Ninth International Shock Tube Symposium*, edited by D. Bershader and W. Griffith, Stanford University Press, Stanford, Calif., 1973, pp. 664–667.

[7]Harris, C. J., and Rogers, D. A., "Performance of Electrical Discharge Shock Wave Devices," Report 71SD217, Feb. 1971, General Electric Environmental Sciences Laboratory.

[8]Dannenberg, R. E., "An Imploding Trigger Technique for Improved Operation of Electric Arc Drivers," *Shock Tubes, Proceedings of the Seventh International Shock Tube Symposium*, edited by I. I. Glass, University of Toronto Press, Toronto, Canada, 1970, pp. 186–200.

[9]Elkins, R. T. and Baganoff, D., "A Composite Model for a Class of Electric-Discharge Shock Tubes, " *Recent Developments in Shock Tube Research, Proceedings of the Ninth International Shock Tube Symposium,* edited by D. Bershader and W. Griffith, Stanford University Press, Stanford, Calif., 1973, pp. 652–663.

[10]Leibowitz, L. P., "Attainment of Jupiter Entry Shock Velocities," *AIAA Journal,* Vol. 13, March 1975, pp. 403–404.

[11]Craig, R. A. and Davy, W. C., "Absolute Radiometers for Use in Ballistic-Range and Shock Tube Experiments," TN D-5360, Oct. 1969, NASA.

[12]Dannenberg, R. E., and Humphrey, D. E. "Microsecond Response System for Measuring Shock Arrival by Changes in Stream Electrical Impedance in a Shock Tube," *Review of Scientific Instruments*, Vol. 39, Nov. 1968, pp. 1191–1196.

[13]Warren, W. R. and Harris, C. J., "A Critique of High-Performance Shock Tube Driving Techniques," *Proceedings of the Seventh International Shock Tube Symposium*, edited by I. I. Glass, University of Toronto Press, Toronto, Canada, 1970, pp. 143–176.

[14]Olstad, W. B., "Technology Requirement and Experimental Facilities," *Astronautics & Aeronautics*, Vol. 12, Nov. 1974, pp. 58–69.

[15]Miller, C. G., III and Wilder, S. E., "Tables and Charts of Equilibrium Normal Shock and Shock-Tube Solutions for Helium-Hydrogen Mixtures with Velocities to 70 km/sec," NASA SP-3085, 1974.

[16]Boruchi, W. J., "Kerr-Cell-Shuttered f/1.5 Stigmatic Spectrograph for Nano-second Exposures," *Applied Optics*, Vol. 9, Feb. 1970, pp. 259–264.

[17]Boruke, W. J., Cooper D. M., and Page, W. A., "Instrumentation for Measuring Flow Properties in an Explosively Driven Shock Tube," *Proceedings of the Seventh International Shock Tube Symposium*, edited by I. I. Glass, University of Toronto Press, Toronto, Canada, 1970, pp. 707–720.